Mechanofluorochromism of pyrenyl acrylates with different substitutional position and steric hindrance

Yuichi Hirai, Anna Wrona-Piotrowicz, Janusz Zakrzewski, Arnaud Brosseau, Rémi Métivier, Clémence Allain

Journal Pre-proof

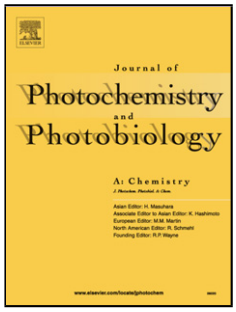

Mechanofluorochromism of pyrenyl acrylates with different substitutional position and steric hindrance

Yuichi Hirai (Conceptualization) (Investigation) (Visualization) (Writing - original draft), Anna Wrona-Piotrowicz (Investigation), Janusz Zakrzewski (Conceptualization), Arnaud Brosseau (Resources) (Validation), Rémi Métivier (Conceptualization) (Supervision) (Writing - review and editing), Clémence Allain (Conceptualization) (Supervision) (Writing - review and editing) (Funding acquisition)

PII: S1010-6030(20)30769-3

DOI: https://doi.org/10.1016/j.jphotochem.2020.112972

Reference: JPC 112972

To appear in: *Journal of Photochemistry & Photobiology, A: Chemistry*

Received Date: 27 May 2020

Revised Date: 30 September 2020

Accepted Date: 9 October 2020

Please cite this article as: Hirai Y, Wrona-Piotrowicz A, Zakrzewski J, Brosseau A, Métivier R, Allain C, Mechanofluorochromism of pyrenyl acrylates with different substitutional position and steric hindrance, *Journal of Photochemistry and amp; Photobiology, A: Chemistry* (2020), doi: https://doi.org/10.1016/j.jphotochem.2020.112972

Mechanofluorochromism of pyrenyl acrylates with different substitutional position and steric hindrance

Yuichi Hirai,[a] Anna Wrona-Piotrowicz,[b] Janusz Zakrzewski,[b] Arnaud Brosseau,[a] Rémi Métivier*[a] and Clémence Allain*[a]

[a] PPSM, CNRS, ENS Paris-Saclay, 61 Avenue du Président Wilson, 94230, Cachan, France

E-mail: remi.metivier@ens-paris-saclay.fr, clemence.allain@ens-paris-saclay.fr

[b] Department of Organic Chemistry, Faculty of Chemistry, University of Łódź, Tamka 12, 91-403 Łódź, Poland

Graphical abstract

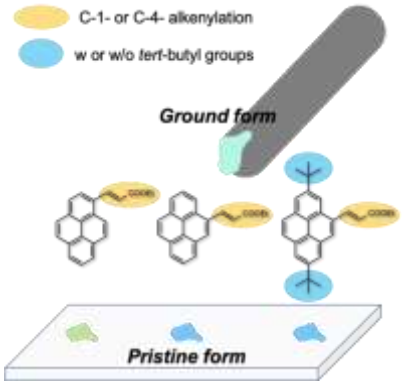

Highlights:

- Mechanofluorochromism (MFC) is reported for pyrenyl acrylates.
- The C-1- and C-4-alkenylated pyrenes exhibited hypsochromic and bathochromic MFC.
- Bulky groups in 2,7-position reduced the molecular rearrangement after grinding.
- MFC of pyrene-derived acrylates is discussed based on emission spectra and decay times.

Abstract:

Solid-state emission color change upon mechanical stimuli, known as mechanofluorochromism (MFC), is reported for pyrenyl acrylates. The C-1- and C-4-alkenylated pyrenes ((*E*)-Ethyl-3-(Pyren-1-yl)acrylate and (*E*)-Ethyl-3-(Pyren-4-yl)acrylate, respectively) exhibited distinct MFC behaviors (hypsochromic and bathochromic shifts). The introduction of bulky *tert*-butyl groups in 2,7-position ((*E*)-Ethyl-3-(2,7-Di-tert-butylpyren-4-yl)acrylate) also induced the shifted overlapping of pyrene moiety in pristine form and suppressed the thermal back reaction in ground form. These characteristic MFC behaviors of pyrene-derived acrylates are discussed on the basis of emission spectra and decay times in pristine and ground forms.

Keywords: solid-state luminescence • pyrene dye • organic materials • mechanofluorochromism • polymorphism

Introduction:

Emission color change upon mechanical stimulation, so-called mechanofluorochromism (MFC), and has attracted attention especially in the last ten years. A growing number of MFC molecules including organic and organometallic compounds has been reported,[1-6] and stress-sensitive dyes/polymer composites have also been developed as MFC materials.[7,8] Fluorescent planar cores with mobile branches, such as π-aromatic systems with rotational alkyl groups, are generally recognized as promising chemical structures to host MFC properties. Our groups have explored the synthetic diversity of pyrene derivatives and demonstrated the fluorescence properties both in solution and in the solid state.[9-12] The solid-state fluorescence of pyrene derivatives is getting more common recently, and several examples of MFC with planar/branch structural features have been reported.[13-18] Therefore, it is of great interest to establish a new library of organic MFC materials by investigating their dynamic photophysical properties in solid state. As a series of our reported pyrene derivatives, we here focused on C-1- and C-4-alkenylated pyrenes with and without *tert*-butyl groups for their solid-state blue/green fluorescence properties up to 0.35 quantum yields.[11] Since these fluorescent molecules bear a planar unit with chain-like side groups, the emission color change is expected to be accompanied by intermolecular arrangement changes. In addition, systematic MFC study on the

compounds w/ and w/o specific chemical groups and positional isomers would provide a clue to correlate the steric structures and MFC properties.

We here report the MFC of C-1- and C-4-alkenylated pyrenes ((*E*)-Ethyl-3-(Pyren-1-yl)acrylate: **1**, (*E*)-Ethyl-3-(Pyren-4-yl)acrylate: **2**, respectively) to investigate the positional effect of substituents on mechanical properties. C-4-Alkenylated pyrene with *tert*-butyl groups in 2,7- positions ((*E*)-Ethyl-3-(2,7-Di-tert-butylpyren-4-yl)acrylate: **3**) is also introduced to investigate the steric effect on MFC properties. The target molecules were prepared following the reported synthetic methods.[11] As-synthesized powder samples are defined as pristine condition. To study the spectroscopy of the ground form, a quartz plate was directly scratched with a pestle immediately after grinding of the powder (Figure 1). Photophysics in the solid state has been reinvestigated compared to our previous work to take into account the mechanofluorochromism of these compounds and their solid-state back reactions.

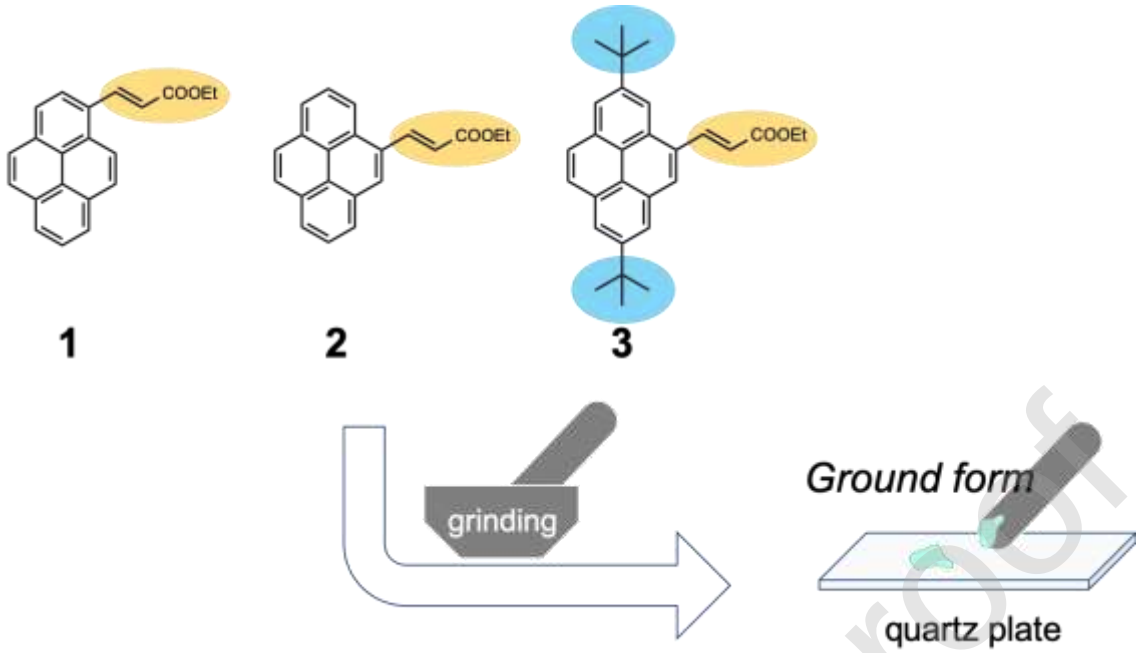

Figure 1. Chemical structures and an illustration of sample preparation of ground pyrene-derived acrylates (**1-3**) for spectroscopy.

Results and Discussion:

In order to gain insights on the molecular electronic transitions responsible for light absorption in this series of compounds, we performed DFT and TD-DFT calculations on **1-3** at the B3LYP/6-31+G(d,p) level of theory using an implicit IEFPCM solvent model for $CHCl_3$. The electronic transitions and corresponding involved molecular orbitals of **1-3** in chloroform solution calculated by time-dependent DFT are depicted in Figure 2, Figure S1 and Table S1 (Supporting Information). For the frontier molecular orbitals HOMO and LUMO, the electron density is not only localized on pyrene but also on the acrylate group. The C-1/C-4 substitutional positions show different π-conjugation of the

acrylic chain with the pyrenyl moiety of **1** and **2**, and *tert*-butyl groups at 2,7- positions slightly vary the electron density distribution of **2** and **3**. For the three compounds, the first electronic transition $S_0 \rightarrow S_1$ corresponds to a HOMO→LUMO transition, associated with a high oscillator strength. Comparison of the data for the three compounds corroborate the lowest energy absorption band of **1** and similar photophysical properties between **2** and **3** observed for isolated molecules in $CHCl_3$.[11]

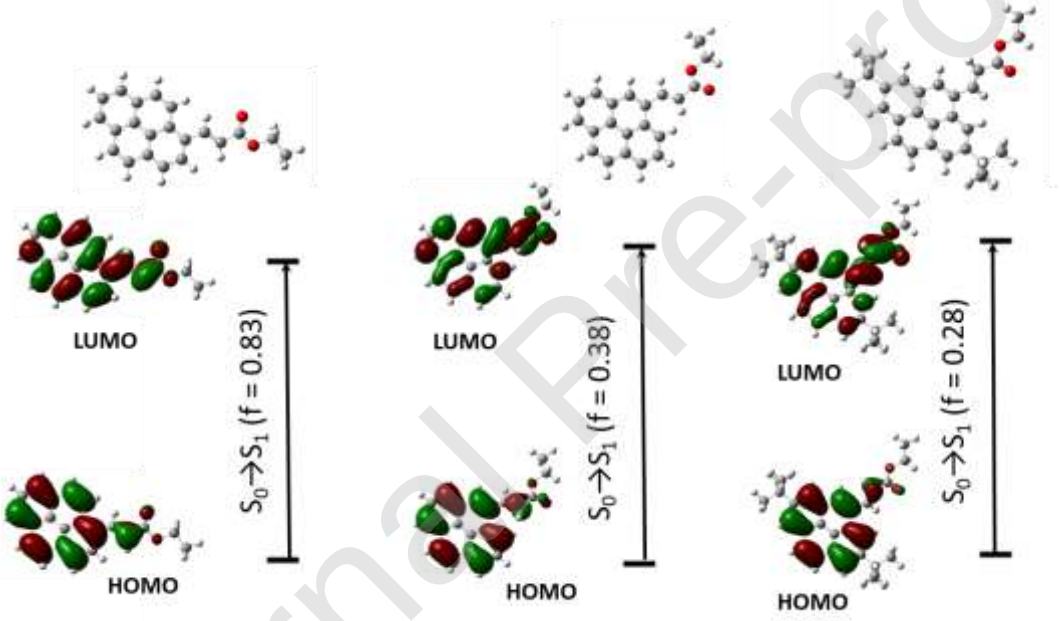

Figure 2. Optimized geometry and HOMO and LUMO orbitals involved in the S_0-S_1 transitions for compounds **1** (left), **2** (middle) and **3** (right), obtained by DFT and TD-DFT calculations at the B3LYP/6-31+G(d,p) level (IEFPCM $CHCl_3$ solvent model).

The solid-state excitation/emission spectra of **1-3** are summarized in Figure 3. Green or blue fluorescence of pristine **1-3** is observed as reported before (Figure 3, black line). Upon mechanical grinding, all of these compounds were found to show MFC (Figure 3,

blue line). In order to take into account the spectral shape modification upon mechanical stimulation, fluorescence color change was estimated using the mean wavelength shift ($\Delta\lambda = \lambda_{mean,ground} - \lambda_{mean,pristine}$, $\Delta\lambda < 0$: hypsochromic shift, $\Delta\lambda > 0$: bathochromic shift) with λ_{mean} defined by equation (1):

$$\lambda_{mean} = \frac{\int_0^\infty \lambda \times I_F(\lambda) d\lambda}{\int_0^\infty I_F(\lambda) d\lambda}, \quad (1)$$

where $I_F(\lambda)$ is the intensity of the emission spectra. The difference of the mean wavelengths before and after grinding is estimated to be $\Delta\lambda = -22$, +28 and +18 nm ($\Delta\nu = +750, -1050, -650$ cm^{-1}) for **1**, **2** and **3**, respectively (Table 1). According to the crystal information file (CIF),[11] **1** forms strong intermolecular interactions due to the close face-to-face π-π stacking (< 3.5 Å) and small distances between the center of gravity in neighboring parallel pyrene units ($d_{center\text{-}center}$ = 4.02 Å), which represents the large overlapping of pyrene moieties (see Figure S2 in Supporting Information). The hypsochromic shift of **1** upon grinding can be explained by the isolation of these molecules with decreased intermolecular interactions.[19] On the other hand, **3** avoids overlapping of the *tert*-butyl groups, resulting in larger distances between pyrene units ($d_{center\text{-}center}$ = 6.19 Å). New intermolecular interactions created upon grinding may cause the bathochromic MFC of **2** and **3**.[20,21] When comparing the relative contribution of two excitation bands in visible (425-450 nm) and ultraviolet regions (~ 360 nm), which were

attributed to the aggregated and monomer conformations in the ground state, respectively,[11] the former is less pronounced after mechanical grinding than in pristine form. Therefore, the aggregated conformers such as preformed dimers in the ground state of pristine forms is partially dislocated by mechanical grinding.

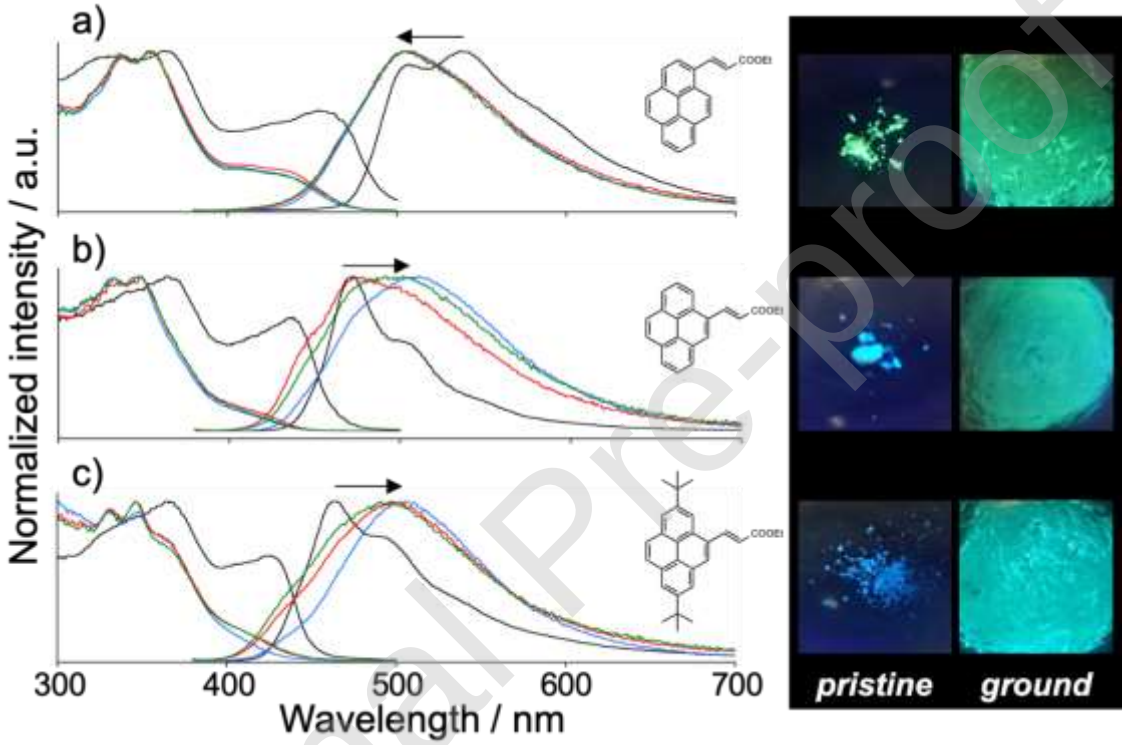

Figure 3. Excitation/emission spectra of a) **1**, b) **2** and c) **3** in solid state (black: pristine, blue: ground, red: 30 min after grinding at RT, green: another 30 min at 50˚C, λ_{ex} = 360 nm, λ_{obs} = 520 nm), and corresponding pictures of pristine/ground forms under UV irradiation (λ_{ex} = 365 nm). Arrow indicates the shift upon mechanical grinding.

Table 1. Sample state and corresponding mean emission wavelength

Sample state[a]	**1**	**2**	**3**
Pristine / nm	557	500	506
Ground / nm	535	528	524
30 min at RT /nm	537	514	519
30min at RT + 30min at 50°C /nm	534	522	518
Total shift $\Delta\lambda$ at RT[b] /nm	−22	+28	+18

[a] All samples were treated at room temperature. [b] Total shift $\Delta\lambda = \lambda_{mean,ground} - \lambda_{mean,pristine}$.

Since the fluorescence color recovery was observed for **2** and **3**, we followed the back reaction behavior to consider the molecular rearrangement in solid state (Figure 3 and Table 1). The ground samples were let sit at room temperature for 30 min (Figure 3, red line) and at 50˚C for another 30 min (Figure 3, green line), and the corresponding emission spectra were recorded to consider the solid-state back reactions. The little spectral change in **1** at room temperature and at 50˚C indicates the existence of another stable and relaxed conformation with reduced intermolecular interactions. On the contrary, the main emission band of the pristine form of **2** (~ 470 nm) recovers in 30 min at room temperature and the relative contribution of the emission bands at 510 nm decreases at the same time. Further heating at 50˚C gives an intermediate spectrum between ground form (blue line) and 30 min after grinding at room temperature (red line). **3** showed limited back reaction at room temperature and another 30 min of heating at 50˚C gave additional spectral shift; however, the original spectral profile was not recovered.

Therefore, the bulky *tert*-butyl groups are considered to hinder the rearrangement of the original molecular conformation in solid state.

For further investigation of the photophysical properties, time-resolved fluorescence measurements of **1-3** were conducted at three distinct emission wavelengths. The fluorescence decays in pristine form were re-measured by using a quartz cell with 0.2 mm-deep hole in order to avoid any mechanical stimulation. Global analysis was successfully converged using a discrete multi-exponential decay model for all sets of three decays of each sample. The estimated lifetimes τ, corresponding pre-exponential factors a and fractions of intensity f are summarized in Table 2 (see Table S3 in supporting information for full sets of data).

Four components were necessary to fit the fluorescence decays at any emission wavelengths for **1-3**. Despite more sophisticated models exist, such as distributions of decay times which may cover the wide variety of molecular species and packings modes,[22] we decided to adopt a sum of four discrete exponentials to fit the obtained decay curves, since this robust model gave satisfactory fits and provided useful information about the excited-state kinetics of **1-3**.

Table 2. Emission decay time-constants (τ) and corresponding pre-exponential factors (a) and fraction of intensity (f). (λ_{ex} = 360 nm, λ_{em} = 530/500 nm for **1**, λ_{em} = 500/500 nm for **2**, λ_{em} = 500/510 nm for **3**, in solid state before/after grinding). * shows a small component (absolute value < 0.01) required to obtain a satisfactory fit.

	τ_1 (a_1, f_1)	τ_2 (a_2, f_2)	τ_3 (a_3, f_3)	τ_4 (a_4, f_4)
1 pristine	12 (0.13, 0.26)	5.6 (0.76, 0.70)	2.5 (0.11, 0.04)	0.85 (−0.17, −0.02)
1 ground	26 (0.03, 0.17)	9.3 (0.29, 0.54)	3.1 (0.43, 0.26)	0.46 (0.25, 0.02)
2 pristine	11 (0.02, 0.05)	4.4 (0.51, 0.68)	2.1 (0.43, 0.27)	0.15 (0.05, *)
2 ground	23 (0.04, 0.26)	8.0 (0.20, 0.47)	2.1 (0.36, 0.21)	0.41 (0.40, 0.05)
3 pristine	8.4 (*, 0.06)	3.1 (0.15, 0.40)	1.3 (0.35, 0.39)	0.33 (0.49, 0.14)
3 ground	28 (0.14, 0.35)	13 (0.44, 0.54)	4.1 (0.27, 0.10)	0.61 (0.15, *)

Before grinding, the fast decay components of **2** and **3** ($\tau \leq 4.4$ ns) correspond to the vast majority of emitting species ($a_2 + a_3 + a_4 = 0.99$) and fluorescence intensity ($f_2 + f_3 + f_4 \geq 0.93$), which represents the blue-emitting monomers due to the larger proportion in shorter wavelength. On the other hand, relatively large contribution of longer decay lifetime (τ_1 = 12 ns) accompanying a fast decay component (τ_4 = 0.85 ns) with a negative pre-exponential factor (a_4 = −0.17) is recognized for **1**, which represents the dynamic excimer formation. Preformed aggregates caused the large contribution of τ_2 (5.6 ns) in

the red part of the spectrum (f_2 = 0.52-0.75 at λ_{em} = 500-560 nm). Much longer emission decay-times (τ = 26, 23 and 28 ns for **1**, **2** and **3**, respectively) appear after mechanical grinding without detectable rise times (eventually with rise times much shorter than the time-resolution of our instrument), which indicates the formation of another excited species such as preformed excimers. The two short components (τ_3 and $\tau_4 \leq 3.1$ ns), appearing as rise times at longer emission wavelength in the pristine form of **1**, contribute as decay times in its ground form. It would be related to the decreased intermolecular interactions as already mentioned. Two short components of **2** and **3** (τ_3 and τ_4, pristine form) arising from the blue-emitting monomers are also identified after grinding. Because of the remained shoulder bands in shorter wavelengths and the fast back reaction after grinding (Figure 3b and 3c, blue lines), the formation of aggregated molecules would be partially and temporarily allowed for **2** and **3**, which was initially in monomeric conformation with large dislocation between neighbouring pyrene units. The further red-shifted emission spectra of molten samples without shoulder bands (Figure S4b and S4c in Supporting Information, black lines) also support that the mechanical grinding does not fully convert the molecular arrangements.

Interestingly, a blue-emissive powder of **1** was also identified by fast recrystallization from dichloromethane, which showed similar fluorescence as pristine **2** and **3** with

structured narrow emission bands at around 470 nm (Figure 4b black line). The as-mentioned sample with green fluorescence is described as **1-green**, and the newly found blue-fluorescent form is denoted as **1-blue** hereafter. Unfortunately, the quality of crystals for **1-blue** was not enough to perform single crystal X-ray analysis. According to the powder X-ray diffraction (XRD) measurements, **1-green** was identified as previously reported orthorhombic crystal system with strong π-π interactions, while **1-blue** showed distinct diffraction patterns (Figure 4d).

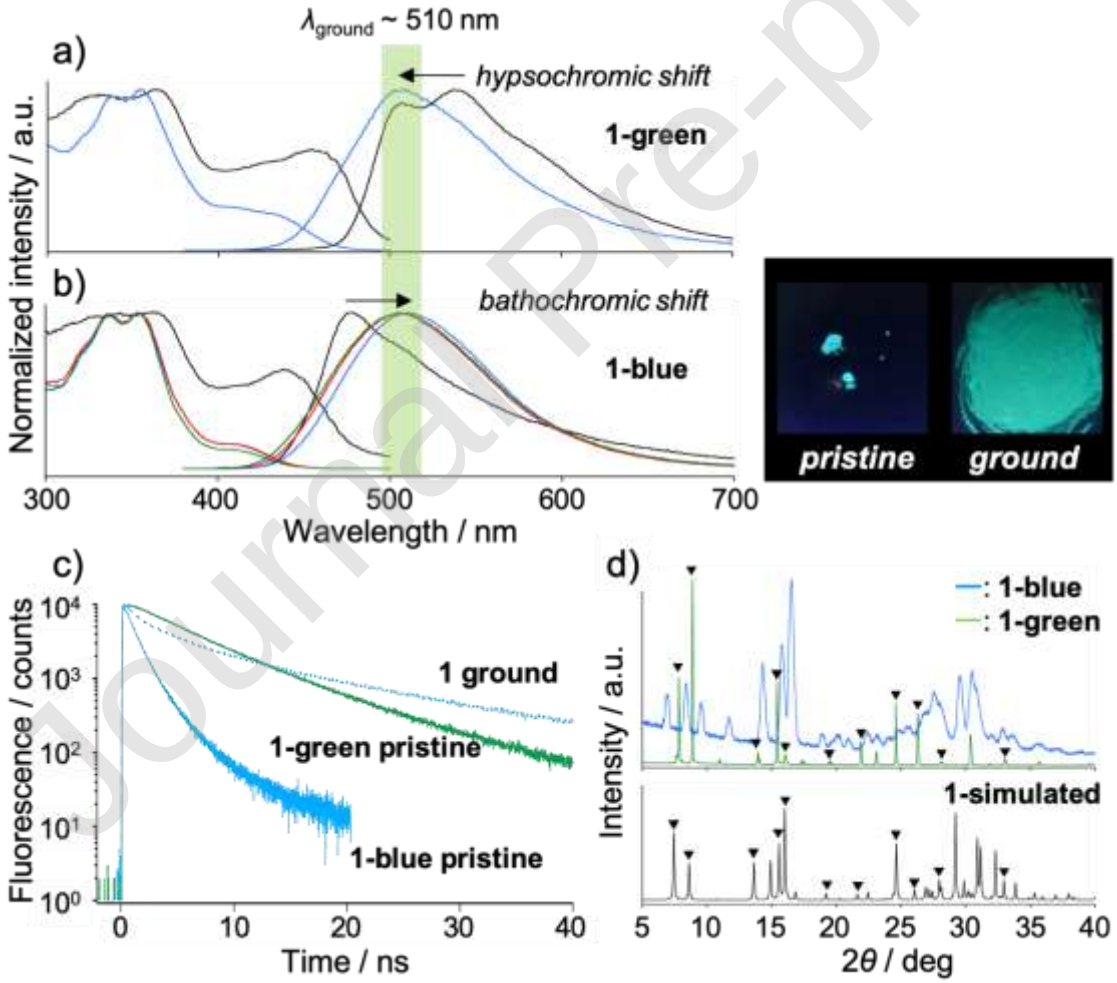

Figure 4. Excitation/emission spectra of a) **1-green** and b) **1-blue** (λ_{ex} = 360 nm, λ_{obs} =

520 nm, black: pristine, blue: ground, red: 30 min after grinding at RT, green: another 30 min at 50˚C), and corresponding pictures of pristine/ground forms under UV irradiation (λ_{ex} = 365 nm). c) Fluorescence decay curves of **1-blue** pristine (λ_{em} = 480 nm, solid blue line), **1-green** pristine (λ_{em} = 530 nm, solid green line) and **1** ground (λ_{em} = 510 nm, dashed blue line) excited at 360 nm. d) Experimental powder X-ray diffraction patterns of **1-blue** (blue line) and **1-green** (green line), and simulated one (black line) of **1** based on the previously reported CIF file (Co tube, λ = 1.79026 Å).[11]

Contrary to the constant contribution of the longest decay-time (τ_1 = 12 ns) of pristine **1-green** at all emission wavelengths, the longest component (τ_1 = 9.2 ns) of pristine **1-blue** is more dominant at longer λ_{em} region but still in minor fraction of intensity (see Table S4 in Supporting Information). The contribution of the shorter components (≤ 2.4 ns) also decrease when λ_{em} increases (f = 0.98 and 0.82 at 450 and 510 nm, respectively). Thus, **1-blue** may be dominated by the blue-emitting monomer with a small fraction of preformed aggregated form as is the same for **2** and **3** in pristine form. Therefore, the crystal packing structures of **1-blue**, **2** and **3** are expected to be similar with small contribution of face-to-face contacts, and the preformed-aggregated-like molecules would be formed under the condition of grinding. Indeed, **1-blue** exhibited bathochromic shift under grinding like **2** and **3**, and the structureless spectral profile centered at around 510 nm is also quite similar to that of **1-green** in ground form (Figure 4, highlighted with green bar). The original fluorescence of **1-blue** was not recovered due to the slight

thermal back reaction at room temperature, and further heating at 50˚C (Figure 4, green line) didn't accelerate the back reaction anymore. The emission lifetimes and even the contribution of emitting species and the fraction of intensity exhibited quite similar trends among these polymorphs in ground form (Table S4 and Figure 4c). Therefore, **1-green** and **1-blue** are considered to form the same metastable conformations in amorphous phase, whatever the initial structure is. The series of pyrene derivatives potentially possess metastable molecular conformations close to the forms obtained by mechanical grinding, which has also been described as polymorphs-driven MFC in some studies.[23-25] We here summarize the results by categorizing the properties into three types; i) blue form (**1-blue**, **2-3** pristine) dominated by monomers (short $\tau \leq 4.4$ ns) and minor proportion of preformed aggregates, ii) green form (**1-green**) which allows the formation of dynamic excimers with rise-times ($a < 0$) and iii) ground form (**1-3** ground) with randomized monomers and long-lived dimers ($\tau \geq 23$ ns).

Conclusions:

In conclusion, we reported the mechanofluorochromism of pyrene-derived acrylates. C-4-alkenylated pyrene (**2**) and one with bulky *tert*-butyl groups in 2,7-position (**3**) showed monomer-like emission in pristine form due to the lack of columnar face-to-face stacking.

The bathochromic shift of these compounds upon grinding indicated the increased intermolecular interactions. C-1-alkenylated pyrene was found to form two types of polymorphs (**1-blue** and **1-green**) with monomer-like and dynamic-excimer-like emission in pristine condition. A pair of bathochromic and hypsochromic shift upon grinding resulted in quite similar spectroscopic features with slight back reactions which suggested the same metastable conformation in amorphous phase whatever the starting state. Further investigation based on crystallography would greatly advance these MFC studies in terms of fundamental understandings and molecular designs for colour-controlled MFC.

Experimental Section

Compounds **1-3** were synthesized and purified according to the earlier published procedure.[11] Pristine powders were prepared by repeated crystallization from hexanes (**1-green**) and evaporation of the dichloromethane solutions obtained by chromatography (**2** and **3**), respectively.

Optical Measurements: Emission and excitation spectra of pristine powder samples were recorded on a HORIBA Jobin-Yvon Fluorolog FL3-221 spectrometer using a short path length optical quartz cell (20/C/Q/0.2, Starna), and the spectra were corrected for the

response of the detector system. The pristine powder was ground using an agate mortar, and the resulting amorphous solid adhered on a pestle surface was immediately transferred to a quartz plate to record the spectra and minimize the effect of back reaction at room temperature. Fluorescence decay profiles were obtained by time-correlated single-photon counting (TCSPC) method with titanium:sapphire laser (Tsunami, Spectra-Physics) pumped by a doubled Nd:YVO4 laser (Millennia Xs, Spectra-Physics). Light pulses at 720 nm was selected by an acousto-optic crystal at a repetition rate of 4 MHz, and then doubled at 360 nm by nonlinear crystals. Fluorescence photons were detected at 90˚ through a polarizer at the magic angle and monochromator, by means of a Hamamatsu MCP R3809U photomultiplier, connected to a SPC-630 TCSPC module from Becker&Hickl. The instrumental response function was recorded before each decay measurement with a fwhm (full width half maximum) of 860 ps. The fluorescence data were analyzed using the Globals software package developed at the Laboratory for Fluorescence Dynamics at the University of California, Irvine, which includes reconvolution analysis and global non-linear least-squares minimization method.

Crystallography: Powder XRD patterns were recorded on a Bruker D2 PHASER with a Si single crystal plate (Co tube, λ = 1.79026 Å).

Computational calculations: The geometry of compounds **1-3** was fully optimized using

the Becke-3-Lee-Yang-Parr (B3LYP)[26] exchange functional with the 6-31+G(d,p) basis set, including IEFPCM solvent model for $CHCl_3$, as implemented in the Gaussian 16 software package, Revision B.01.[27] The absence of negative frequencies was checked to ensure true energy minima. Franck-Condon energy transitions, oscillator strengths, and involved molecular orbitals were calculated using the time-dependent DFT formalism (TD-DFT) with the same functional and basis set.

DSC measurements were performed on a DSC 25 Discovery series (TA Instruments) instrument, with a 10°C/min scan rate.

CRediT author statement

Yuichi Hirai: Conceptualization, Investigation, Visualization, Writing - Original Draft

Anna Wrona-Piotrowicz: Investigation

Janusz Zakrzewski: Conceptualization

Arnaud Brosseau: Resources, Validation

Rémi Métivier: Conceptualization, Supervision, Writing - Review & Editing

Clémence Allain: Conceptualization, Supervision, Writing - Review & Editing, Funding acquisition

Declaration of interests

The authors declare that they have no known competing financial interests or personal relationships that could have appeared to influence the work reported in this paper.

Acknowledgements

We would like to appreciate Dr. Pasko Oleksandr (SATIE, CNRS ENS Paris-Saclay) for the powder X-ray diffraction measurements, and Laurent Michely and Dr. Davy-Louis Versace (ICPME, Thiais) for the DSC measurements. Y. H. gratefully acknowledges support from the Japan Society of the Promotion of Science (JSPS). R.M. and C. A. acknowledge ERC funding 'MECHANO-FLUO' (St-G 715757) project. This work was performed using HPC resources from the "Mésocentre" computing center of CentraleSupélec and École Normale Supérieure Paris-Saclay supported by CNRS and Région Île-de-France (http://mesocentre.centralesupelec.fr/).

References:

[1] R. Gawinecki, 4-Tert-Butyl-1-(4'-dimethylamino-benzylideneamino)pyridinium Perchlorate (BDPP): A Novel Fluorescent Dyes, Dyes Pigm. 28 (1993), 73-78. https://doi.org/10.1016/0143-7208(93)80026-W.

[2] Y. Sagara, S. Yamane, M. Mitani, C. Weder, T. Kato, Mechanoresponsive

Luminescent Molecular Assemblies: An Emerging Class of Materials, Adv. Mater. 28 (2016), 1073–1095. https://doi.org/10.1002/adma.201502589.

[3] K. Nagura, S. Saito, H. Yusa, H. Yamawaki, H. Fujihisa, H. Sato, Y. Shimoikeda, S. Yamaguchi, Distinct Responses to Mechanical Grinding and Hydrostatic Pressure in Luminescent Chromism of Tetrathiazolylthiophene, J. Am. Chem. Soc. 135 (2013), 10322–10325. https://doi.org/10.1021/ja4055228.

[4] P. S. Hariharan, N. S. Venkataramanan, D. Moon, S. P. Anthony, Self-Reversible Mechanochromism and Thermochromism of a Triphenylamine-Based Molecule: Tunable Fluorescence and Nanofabrication Studies, J. Phys. Chem. C 119 (2015), 9460–9469. https://doi.org/10.1021/acs.jpcc.5b00310.

[5] C. J. Lin, Y. H. Liu, S. M. Peng, T. Shinmyozu, J. S. Yang, Excimer-Monomer Photoluminescence Mechanochromism and Vapochromism of Pentiptycene-Containing Cyclometalated Platinum(II) Complexes, Inorg. Chem. 56 (2017), 4978–4989. https://doi.org/10.1021/acs.inorgchem.7b00009.

[6] H. Ito, M. Muromoto, S. Kurenuma, S. Ishizaka, N. Kitamura, H. Sato, T. Seki, Mechanical Stimulation and Solid Seeding Trigger Single-Crystal-to-Single-Crystal Molecular Domino Transformations, Nat. Commun. 4 (2013), 1–5. https://doi.org/10.1038/ncomms3009.

[7] B. R. Crenshaw, C. Weder, Deformation-Induced Color Changes in Melt-Processed Photoluminescent Polymer Blends, Chem. Mater. 15 (2003), 4717–4724. https://doi.org/10.1021/cm034447t.

[8] C. Calvino, L. Neumann, C. Weder, S. Schrettl, Approaches to Polymeric Mechanochromic Materials, J. Polym. Sci. Part A Polym. Chem. 55 (2017), 640–652. https://doi.org/10.1002/pola.28445.

[9] R. Flamholc, D. Plazuk, J. Zakrzewski, R. Métivier, K. Nakatani, A. Makal, K. Woźniak, A New Class of Pyrenyl Solid-State Emitters: 1-Pyrenyl Ynones. Synthesis via the Friedel-Crafts Route, Molecular and Electronic Structure and Photophysical Properties, RSC Adv. 4 (2014), 31594–31601. https://doi.org/10.1039/c4ra03961k.

[10] A. Wrona-Piotrowicz, J. Zakrzewski, R. Métivier, A. Brosseau, A. Makal, K. Woźniak, Efficient Synthesis of Pyrene-1-Carbothioamides and Carboxamides. Tunable Solid-State Fluorescence of Pyrene-1-Carboxamides, RSC Adv. 4 (2014), 56003–56012. https://doi.org/10.1039/c4ra07045c.

[11] M. Piotrowicz, J. Zakrzewski, R. Métivier, A. Brosseau, A. Makal, K. Woźniak, Aerobic Palladium(II)-Catalyzed Dehydrogenative Heck Reaction in the Synthesis of Pyrenyl Fluorophores. A Photophysical Study of β-Pyrenyl Acrylates in

Solution and in the Solid State, J. Org. Chem. 80 (2015), 2573–2581. https://doi.org/10.1021/jo502619k.

[12] A. Wrona-Piotrowicz, J. Zakrzewski, A. Gajda, T. Gajda, A. Makal, A. Brosseau, R. Métivier, Friedel-Crafts-Type Reaction of Pyrene with Diethyl 1-(Isothiocyanato)Alkylphosphonates. Efficient Synthesis of Highly Fluorescent Diethyl 1-(Pyrene-1-Carboxamido)Alkylphosphonates and 1-(Pyrene-1-Carboxamido)Methylphosphonic Acid, Beilstein J. Org. Chem. 11 (2015), 2451–2458. https://doi.org/10.3762/bjoc.11.266.

[13] Y. Sagara, T. Mutai, I. Yoshikawa, K. Araki, Material Design for Piezochromic Luminescence: Hydrogen-Bond-Directed Assemblies of a Pyrene Derivative, J. Am. Chem. Soc. 129 (2007), 1520–1521. https://doi.org/10.1021/ja0677362.

[14] Y. Sagara, T. Kato, Stimuli-Responsive Luminescent Liquid Crystals: Change of Photoluminescent Colors Triggered by a Shear-Induced Phase Transition, Angew. Chemie - Int. Ed. 47 (2008), 5175–5178. https://doi.org/10.1002/anie.200800164.

[15] S. Ito, G. Katada, T. Taguchi, I. Kawamura, T. Ubukata, M. Asami, Tricolor Mechanochromic Luminescence of an Organic Two-Component Dye Visualization of a Crystalline State and Two Amorphous States, CrystEngComm 21 (2019), 53–59. https://doi.org/10.1039/c8ce01698d.

[16] Z. Ma, M. Teng, Z. Wang, S. Yang, X. Jia, Mechanically Induced Multicolor Switching Based on a Single Organic Molecule, Angew. Chemie - Int. Ed. 52 (2013), 12268–12272. https://doi.org/10.1002/anie.201306503.

[17] Y. Sagara, T. Komatsu, T. Ueno, K. Hanaoka, T. Kato, T. Nagano, A Water-Soluble Mechanochromic Luminescent Pyrene Derivative Exhibiting Recovery of the Initial Photoluminescence Color in a High-Humidity Environment, Adv. Funct. Mater. 23 (2013), 5277–5284. https://doi.org/10.1002/adfm.201300180.

[18] Y. Hirai, A. Wrona-Piotrowicz, J. Zakrzewski, A. Brosseau, R. Guillot, R. Métivier, C. Allain, Mechanofluorochromism of Pyrene-Derived Amidophosphonates, Photochem. Photobiol. Sci. 19 (2020), 229–234. https://doi.org/10.1039/c9pp00457b.

[19] K. Suenaga, K. Tanaka, Y. Chujo, Heat-Resistant Mechanoluminescent Chromism of the Hybrid Molecule Based on Boron Ketoiminate Modified Octasubstituted Polyhedral Oligomeric Silsesquioxane, Chem. - A Eur. J. 23 (2017), 1409–1414. https://doi.org/10.1002/chem.201604662.

[20] H. Ito, T. Saito, N. Oshima, N. Kitamura, S. Ishizaka, Y. Hinatsu, M. Wakeshima, M. Kato, K. Tsuge, M. Sawamura, Reversible Mechanochromic Luminescence of [(C6F5Au)2(μ-1,4-Diisocyanobenzene)], J. Am. Chem. Soc. 130 (2008), 10044–

10045. https://doi.org/10.1021/ja8019356.

[21] T. Seki, K. Kashiyama, H. Ito, Luminescent Mechanochromism of Gold N -Heterocyclic Carbene Complexes with Hypso- and Bathochromic Spectral Shifts, Dalt. Trans. 48 (2019), 7105–7109. https://doi.org/10.1039/c9dt00566h.

[22] R. Métivier, I. Leray, M. Roy-Auberger, N. Zanier-Szydlowski, B. Valeur, B. Valeur, Characterization of Alumina Surfaces by Fluorescence Spectroscopy. Part 1. Grafting a Pyrene Derivative on γ- and δ-Alumina Supports, New J. Chem. 26 (2002), 411–415. https://doi.org/10.1039/b109144c.

[23] Q. Qi, J. Zhang, B. Xu, B. Li, S. X. A. Zhang, W. Tian, Mechanochromism and Polymorphism-Dependent Emission of Tetrakis(4-(Dimethylamino)Phenyl)Ethylene, J. Phys. Chem. C 117 (2013), 24997–25003. https://doi.org/10.1021/jp407965a.

[24] Y. Lei, Y. Zhou, L. Qian, Y. Wang, M. Liu, X. Huang, G. Wu, H. Wu, J. Ding, Y. Cheng, Polymorphism and Mechanochromism of N -Alkylated 1,4-Dihydropyridine Derivatives Containing Different Electron-Withdrawing End Groups, J. Mater. Chem. C 5 (2017), 5183–5192. https://doi.org/10.1039/c7tc00362e.

[25] S. Long, S. Parkin, M. A. Siegler, A. Cammers, T. Li, Polymorphism and Phase

Behaviors of 2-(Phenylamino)Nicotinic Acid, Cryst. Growth Des. 8 (2008), 4006–4013. https://doi.org/10.1021/cg800123z.

[26] A. D. Becke, Density-functional thermochemistry. III. The role of exact exchange, J. Chem. Phys. 98 (1993), 5648-5652. https://doi.org/10.1063/1.464913.

[27] M. J. Frisch et al., Gaussian 16, Revision B.01, Gaussian, Inc., Wallingford CT, 2016.